Status of Use of Lunar Irradiance for On-orbit Calibration

Thomas C. Stone[a], Hugh H. Kieffer[a] and James M. Anderson[b]

[a]US Geological Survey, 2255 N. Gemini Dr., Flagstaff, AZ 86001, USA
[b]New Mexico Institute of Mining and Technology
1003 Lopezville Rd., Socorro, NM 87801, USA

ABSTRACT

Routine observations of the Moon have been acquired by the Robotic Lunar Observatory (ROLO) for over four years. The ROLO instruments measure lunar radiance in 23 VNIR (Moon diameter ∼500 pixels) and 9 SWIR (∼250 pixels) passbands every month when the Moon is at phase angle less than 90 degrees. These are converted to exoatmospheric values at standard distances using an atmospheric extinction model based on observations of standard stars and a NIST-traceable absolute calibration source. Reduction of the stellar images also provides an independent pathway for absolute calibration. Comparison of stellar-based and lamp-based absolute calibrations of the lunar images currently shows unacceptably large differences. An analytic model of lunar irradiance as a function of phase angle and viewing geometry is derived from the calibrated lunar images. Residuals from models which fit hundreds of observations at each wavelength average less than 2%. Comparison with SeaWiFS observations over three years reveals a small quasi-periodic change in SeaWiFS responsivity that correlates with distance from the Sun for the first two years, then departs from this correlation.

Keywords: Moon, calibration, irradiance, spacecraft

1. INTRODUCTION

The ROLO lunar radiometry program continues to acquire images of the Moon and stars at 23 VNIR wavelengths, seven of which approximate existing spacecraft wavelengths, and 9 SWIR bands. The VNIR instrument utilizes a 512×512-pixel CCD detector; the SWIR camera is a 256×256 HgCdTe photoconductive array. The telescope optics are designed such that the Moon just fills each detector at its closest approach. A substantial fraction of observing time is devoted to stellar observations, resulting in a database of instrument stellar irradiances with uncertainties ∼1% in the VNIR and ∼2% in the SWIR. The ROLO database currently holds 67505 lunar images and nearly 680 000 star images after culling of observations determined to have been adversely affected by clouds. Analysis of star observations has provided an independent pathway for absolute calibration through photometric measurements of the star Vega. The ground-based calibration system employs a diffuse white plaque illuminated by a NIST-traceable calibrated FEL lamp. Current comparisons between these two calibrations show an unacceptably large difference.

The calibrated lunar images form the basis of an analytic model of lunar irradiance as a function of phase angle and viewing geometry covering the full range of lunar libration. These models fit hundreds of lunar images at each wavelength, resulting in relative uncertainties just over 1%. Lunar irradiances produced by the model have been used to determine trends in spacecraft instrument radiometric responsivity. Comparison with more than 3 years of SeaWiFS observations of the Moon show a periodic variation in the SeaWiFS calibration, initially correlated with the spacecraft heliocentric range.

2. DATA ACQUISITION AND REDUCTION

The ROLO project goals are to provide exoatmospheric radiance images of the Moon at lunar phase within $\pm 90°$. The exoatmospheric correction depends on multiple observations of a subset of 190 selected standard stars throughout each observing night. These stellar observations allow determination of nightly atmospheric extinction coefficients, which are applied in turn to the lunar images. The intensity difference between the Moon and stars is accommodated

Further author information: (Send correspondence to T.C.S.)
e-mail: tstone@flagmail.wr.usgs.gov; voice: 928-556-7381; fax: 928-556-7014
H.H.K.: e-mail: hkieffer@flagmail.wr.usgs.gov; J.M.A.: e-mail: janderso@aoc.nrao.edu
http://wwwflag.wr.usgs.gov/USGSFlag/Space/LunarTel/index.html

by inserting a neutral density filter into the optical path for lunar observations. Lunar images are acquired in all 32 bandpass filters approximately every half hour when the Moon is higher than 30° above the horizon. The remainder of observing time (∼75% when the Moon is in view) is dedicated to the stellar observations.

Processing of the raw images follows well-established techniques for removal of instrumental effects such as detector bias and dark current subtraction, linearity correction, and array flatfielding. The dark current of the VNIR CCD images is predicted from a linear function of dark level versus exposure time. Dedicated dark frames are acquired at the start and end of each observing night to generate a pixel-by-pixel set of linear least-squares fit coefficients to be used for that night. The DC bias level is measured from a 16×512-pixel area of the CCD which has been cleared by a special clocking sequence just prior to readout. Dark current and bias removal for the SWIR images is somewhat more complicated, as the bias level is known to drift up to 10% over the course of a night, likely due to ambient temperature fluctuations affecting the preamps and A/D electronics. These drifts are modeled by a polynomial fit of dark current images which are acquired with each filter wheel cycle throughout the night. Linearity corrections for both detectors are applied on a per-pixel basis using empirical fit coefficients derived from a set of special observations acquired at varying incident light levels. Flatfield correction images are acquired 2 or 3 times each lunation by observing a Spectralon[1] reflectance panel illuminated by a 1000 Watt FEL calibration lamp. These observations are also part of the ROLO ground-based absolute calibration procedures described below. All observational data images are normalized by exposure time to yield instrument response rates in DN/sec.

The stellar observations are further processed to determine object intensities in instrument response units using a numerical aperture photometry scheme. Star signatures are identified as typically the brightest features in the VNIR images. The stellar data reduction algorithm for VNIR images finds the location of the center of luminosity of the target to sub-pixel resolution. A sky background level is calculated by integrating the image intensity within an annulus between 33 and 58 pixels radius from the center. This background level is subtracted from the entire image. The central maximum is then integrated using a radial weighting function which gives full weight out to 4.5 pixels, gradually decreasing to zero at 9 pixels. (A non-steplike weighting function is also used for the background annulus integration.) The SWIR star images are handled somewhat differently, since stellar luminosities in the infrared can be significantly diminished from the visible. Because extraneous stars in the SWIR FOV can appear brighter than the target star, the sky background for subtraction is derived externally and adapted to nightly conditions. Special observations of regions of the sky relatively devoid of bright stars have been acquired over a wide range of ambient temperatures. An analytic function is fitted to these measurements, which is then used to determine the sky background level for the routine observations based on their particular ambient temperature. The centroid position of the target star signature is determined using all SWIR filter bands (nominally 9). The integration weighting function gives full weight out to 2.75 pixels radius, decreasing to zero at 4.25 pixels, in accord with the plate scale being roughly twice that of the VNIR instrument.

The results of the stellar image processing routines are instrument intensities at the detectors given as response rates in DN/sec. These data are stored as binary table files for each night of observations. Data collected and tabulated along with the star and background integrations and their associated uncertainties include the time of observation and the location in the sky in terms of zenith and azimuth angles. These geometric properties define the airmass through which the observations were made.

The stellar intensities and observational geometry are used to derive nightly atmospheric extinction parameters. Details of the method used are found in Ref. 2. The extinction model fits the *abundances* of atmospheric absorbing species, which are allowed to vary smoothly in time over the course of the night. The constituents modeled are the "normal" gases (N_2, O_2, CO_2, etc.), water vapor, and ozone, plus terms for Rayleigh scattering and four aerosol species. Atmospheric transmission profiles were determined from MODTRAN v3.7[3,4] spectra and the 1976 Standard Atmosphere (mid-latitude winter conditions) adapted to a visibility of 200 km to match the Flagstaff mean extinctions in the Strömgren b and y bands (cf. Ref. 5). Through a separate analysis of ∼600 000 ROLO stellar images, exoatmospheric instrument response magnitudes and absolute irradiances for the ROLO standard stars have been determined. Use of these exoatmospheric data in the extinction algorithm allows fitting a nightly variable instrument gain term. Iteration of this process has reduced the stellar irradiance residuals to levels comparable to published astronomical photometric measurements (e.g. Ref. 6). Plots of the stellar residuals are shown in Figure 1.

The stellar extinction routine produces a set of coefficients representing the best fit to the time-dependent atmospheric component abundances. These values are written to a text output file for each night processed, and used in subsequent calculations of extinction corrections for the lunar images. Calculated nightly stellar exoatmospheric

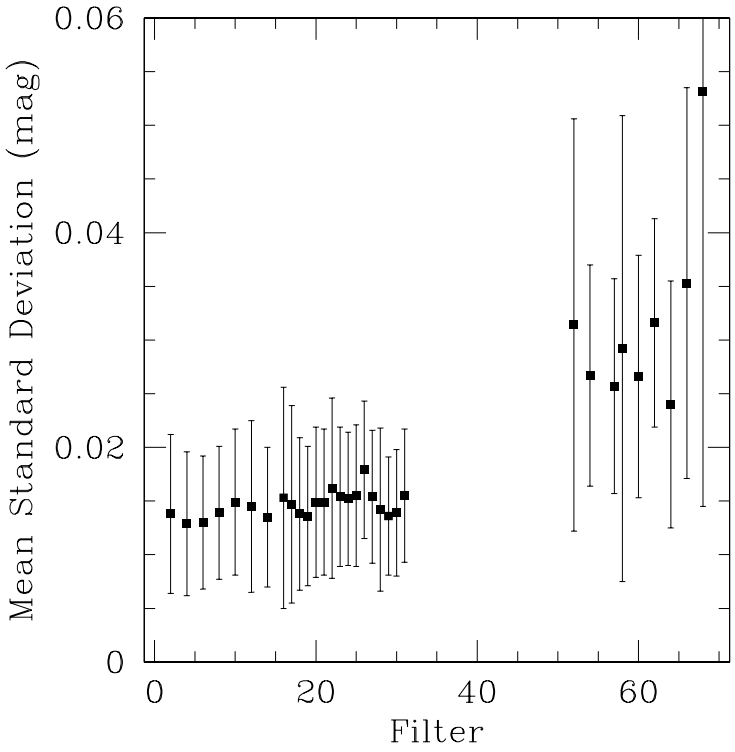

Figure 1. Mean standard deviation in the stellar residuals plotted for each ROLO filter†. Filter wavelengths are given in Table 1. The errorbars represent one standard deviation about the mean residual level for 420 selected nights of data.

irradiances are also written to a separate binary data file along with the stellar viewing geometry. These data are used for ongoing characterizations of the ROLO instrumentation.

Initial reduction of the ROLO lunar images yields an integrated irradiance and the location of the luminous Moon in the frame. The lunar bright limb and selenographic North orientation are known from ephemeris data and the telescope hardware orientation. For each image, the bright limb is fitted to an elliptical curve to determine the center pixel position and "radius" of the Moon image. The pixels within the area defining the Moon are summed, and a sky background level is determined from summing over a superior annular region. These irradiance sums in instrument response units (DN/sec), the centering parameters, and uncertainties for each of these quantities are merged with the image file header information. In final processing the images are projected onto a grid system fixed to selenographic coordinates which covers all of the lunar surface ever visible from Flagstaff. This "Alex" projection is a modified Lambert Azimuthal Equal-Area conformal projection.[7]

Throughout the lunar and stellar data reduction processes a detailed error analysis is conducted. Uncertainty estimates are determined from instrument characterizations and from statistical interrogations of the raw image data. These error estimates are used in the various fitting operations performed as parts of the standard processing.

After each complete data reduction run a table of parameters is built to streamline further analysis. In addition to the observational ancillary data, this table contains calculated geometric relational quantities such as sub-solar and sub-observer selenographic latitude and longitude, results of the standard reductions such as the integrated lunar irradiance sum and sky background level, the radiance calibration constants, and the nightly extinction correction factors, all with corresponding uncertainties. The most recent table build incorporates 67505 individual lunar images, producing a binary-format table file over 34.6 Mb in size. This "Alex table" is the database accessed for the photometric modeling part of the ROLO program.

†Astronomical magnitude $= -2.5 \log_{10}$, relative 0.01 mag is $\sim$1%.

Table 1. ROLO filter wavelengths

	VNIR			SWIR	
Filter ID	λ_{eff} (nm)	FWHM (nm)	Filter ID	λ_{eff} (nm)	FWHM (nm)
2	413.2	12.5	52	944.3	21.5
4	442.4	9.6	54	1062.2	27.1
6	488.1	7.9	57	1246.2	23.3
8	550.4	8.7	58	1542.1	48.6
10	666.7	8.3	60	1637.5	23.4
12	747.1	8.7	62	1985.7	38.5
14	867.7	13.9	64	2134.4	54.7
16	347.3	32.5	66	2257.7	48.2
17	352.6	31.6	68	2391.9	58.2
18	405.0	16.2			
19	415.1	17.8			
20	466.5	20.0			
21	475.8	18.4			
22	545.1	18.8			
23	554.9	18.1			
24	694.8	16.8			
25	705.5	16.7			
26	765.6	16.8			
27	776.5	16.9			
28	875.4	18.4			
29	885.8	16.0			
30	934.8	17.6			
31	945.4	18.8			

3. ABSOLUTE RADIANCE CALIBRATION

The ROLO project radiance calibration efforts currently are undergoing rigorous examination and refinement. Absolute calibration constants are generated via two paths: observations of a diffuse radiance source of known brightness, and reduction of star observations tied to published stellar radiant flux measurements. At the present time the calibration constants determined by these two methods show an unacceptably large difference.

3.1. FEL Lamp Calibration

Routine ROLO operations include regular observations of a Spectralon[1] plaque illuminated by a 1000-Watt FEL lamp. The lamp was purchased with a NIST-traceable irradiance calibration. The Spectralon plaque is illuminated at zero incidence angle a distance of 3.40 m from the lamp filament. The flat panel is 31 cm square, masked to a circular aperture which just fills the telescope FOV. The telescopes view the plaque at emergence angles of 18.8° for VNIR and 19.1° for SWIR. These observations are made 2 or 3 times per month, and also serve as flatfield images for the standard data reduction process. The plaque radiance is validated periodically by direct measurement by NASA/EOS transfer radiometers. These radiometer measurements can be validated to better than 2% accuracy.[8]

A preliminary radiance spectrum is determined from the lamp calibration and the plaque viewing geometry, then scaled to the radiometer measurements using a linear least squares fitting routine. The resulting radiance values are then fitted to a Planck blackbody emission curve using a Marquardt-Levenberg non-linear least squares fitting routine. The free parameters for the fit are an intensity scale a_0, a wavelength-power color term a_1, and the effective color temperature a_2, thus:

$$L_{model} = a_0 \frac{2hc^2}{\lambda^{a_1}\ \lambda^5\ \left(e^{\frac{hc}{\lambda k a_2}} - 1\right)} \tag{1}$$

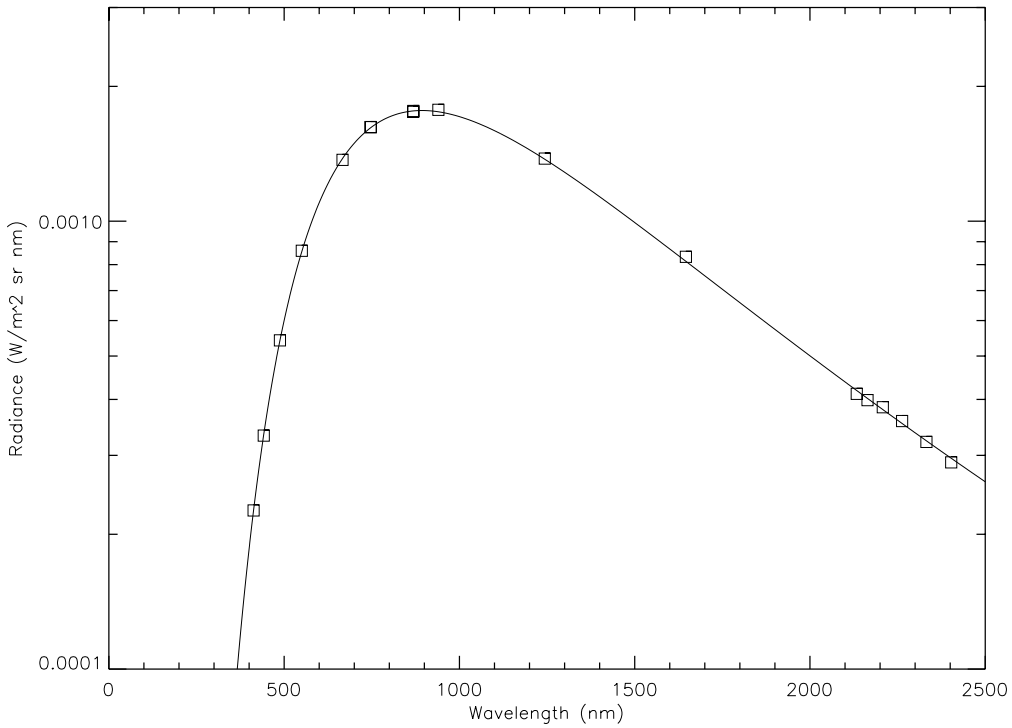

Figure 2. Diffuse Screen Radiance. The symbols show the radiometric validation measurements; the solid line is the synthetic spectrum generated from fitting Equation 1 to the measurement data.

Figure 2 shows the results of this fit. The RMS sum of the measurement differences is 1.06%. The analytic form of Equation 1 is used to generate a synthetic Planck spectrum covering the ROLO wavelength range.

The fitted Planck spectrum is convolved with the ROLO filter transmission curves and a correction for two reflections from aluminum to give the effective radiance in each filter pass band. The images acquired observing the plaque are processed using the ROLO standard reduction routines to remove the instrumental effects of bias level, dark current, non-linearity, and hot/bad pixels. The images are normalized by exposure time; a separate analysis comparing commanded exposure time to detector response has produced an empirical exposure time offset which is applied to all images during the normalization process. Since the telescope FOV is overfilled by the Spectralon target, all pixels in each plaque observation image are summed and averaged to give the instrument response for a band. Dividing the pixel average by the effective bandpass radiance gives the radiometric "responsivity" in units of $(\frac{\mathrm{DN/sec}}{\mathrm{W/m^2 \cdot sr \cdot nm}})$. This quantity is written to the image header. Normalizing each image by the pixel average response produces the flatfield images used in subsequent ROLO processing routines.

3.2. Star Calibration

The ROLO stellar absolute calibration results from comparisons of observations of the star Vega. Observations of Vega have been acquired by the ROLO project for more than four years; analysis of these images has determined the exoatmospheric irradiance of Vega with a current uncertainty estimate less than 1%.

Photometric measurements of Vega found in the astronomical literature[9,10] form the baseline absolute irradiance scale. The synthetic spectrum `veg090250000p.asc49`[11,12] was scaled to the absolute measurement data points and averaged to 0.5 nm resolution. Both the spectrum and measurements were converted to photon flux density units $(\frac{\mathrm{photon}}{\mathrm{sec \cdot m^2 \cdot nm}})$ prior to scaling. The results are shown in Figure 3. This scaled spectrum was convolved with the ROLO filter transmission curves and a correction for two reflections from aluminum to give the effective Vega flux density in each band.

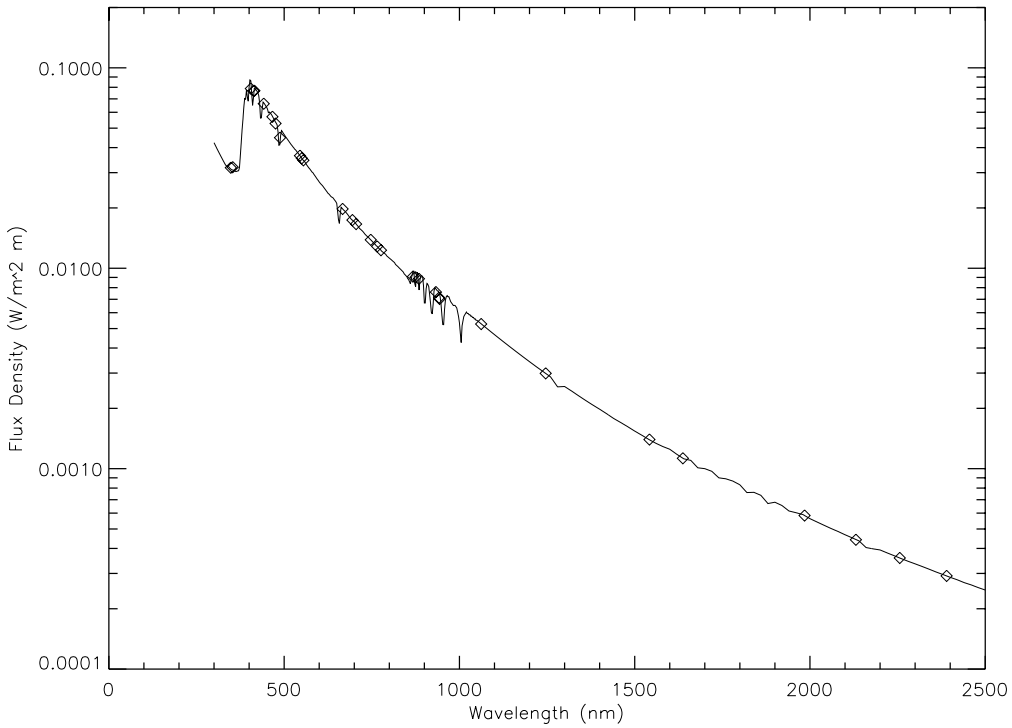

Figure 3. Vega Flux Density. The high-resolution spectrum of Ref. 11 is scaled and averaged to 0.5 nm. The symbols represent the effective flux densities obtained by convolution with ROLO filter passbands.

A separate analysis of all ROLO observations of Vega was conducted to determine a best-fit instrument response. The standard stellar processing algorithm was used to reduce the Vega images to at-telescope irradiance values. The nightly extinction corrections were then applied to convert to exoatmospheric quantities. These data were then closely examined to remove any outlier points which could be attributed to questionable observing conditions. The remaining data were fitted using least-squares analysis to give the best-fit exoatmospheric irradiance in instrument response rate units (DN/sec).

The increased intensity of the Moon requires use of a neutral density filter for lunar observations, while stars are viewed through a fused silica compensator. Since the radiance calibration is applied to the lunar images, the ND filter attenuation is a critical parameter in the stellar calibration determination. Special observations of bright stars are acquired several times a year to measure the ND/compensator ratio. These measurements are fitted to a linear function in time to model the degradation of the filter due to accumulation of dust, etc.

An initial stellar irradiance calibration is determined by converting the Vega photon flux density into energy units ($\frac{\mathrm{W}}{\mathrm{m}^2 \cdot \mathrm{nm}}$) and dividing by the best-fit instrumental irradiance value for each band. The final radiance calibration factors are determined by applying the ND/compensator ratio and dividing by the solid angle of one pixel.

3.3. Calibration Discrepancies

A comparison of the lamp- and star-based calibrations is shown in Figure 4. The scatter in the lamp-based values is probably due to inexact replication of the lamp operating conditions when the validation radiometric measurements were made. The figure shows ROLO filter band 8, centered at 550 nm. The average difference in the two calibrations for this filter is 9.7%.

The stellar calibration plot is identified by the linear trend with time. Because all of the valid ROLO observations of Vega are reduced to a single instrumental irradiance, which is then compared with the published Vega flux spectrum, the calibration factors for each band are constants modified only by the ND/compensator ratio. The two calibrations differ in the VNIR by up to $\sim$36%; the SWIR disparities are somewhat larger.

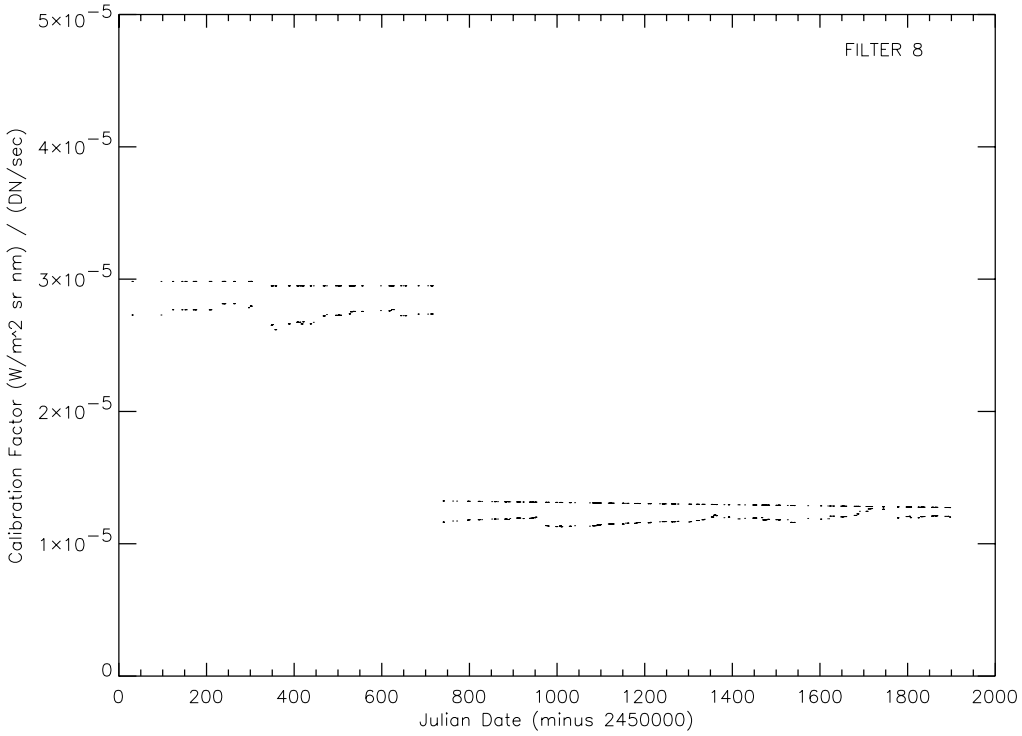

Figure 4. Radiance calibration factors for ROLO filter 8 (550 nm). The FEL/plaque system shows noticeable variations with time, while the Vega-based calibration is linear by definition. The discontinuity near JD 2450740 results from a major overhaul of the telescope optics.

Resolution of these discrepancies is a current priority issue for the ROLO project, proceeding with addressing systematic uncertainties in both calibration systems. The measurements of Vega used to scale the flux spectrum have absolute uncertainty estimates of ∼1.5% in the VNIR[9] and ∼4% in the infrared.[10] Additionally, the transmission passbands of the ROLO filters are not known with the precision of the Vega spectrum, which can lead to errors in the convolution procedure. This effect may be significant in the 488 nm band, which covers the Hβ stellar absorption line at its edge. However, these factors cannot fully account for the observed discrepancy, and do not explain the increased responsivity in the red imposed by the star calibration. The lamp calibration is known to be adversely affected by light scattering problems. Scattering from within the observatory structure during the diffuse source observations was determined to contribute a ∼3–4% measurement error, necessitating modifications to the equipment and procedures. Other deviations from possible scattered light sources currently are being examined. Equipment upgrades are being implemented to stabilize the lamp operating conditions and to directly monitor the diffuse source radiance. An empirical investigation is underway to assess the differences in observing a point source versus a half-degree extended source for absolute calibration.

4. LUNAR IRRADIANCE MODELING

4.1. Data Processing

The Alex table of parameters is built following a full data reduction run; these are conducted at 6–12 month intervals and with release of a new major version of the reduction software. We are currently at version 3. Two Alex tables have been produced from the most recent reduction run, differing primarily in the basis of absolute calibration: table 3.001.0 or 310 is based on the regular FEL/plaque measurements, table 3.001.1 or 311 utilizes the Vega stellar calibration. These two differ significantly, particularly in their overall "color", the 311 version producing a redder lunar albedo spectrum. The ROLO group believes that the discrepancy is due largely to the scattered-light problems associated with the lamp-based calibration system, and currently prefers the 311 model.

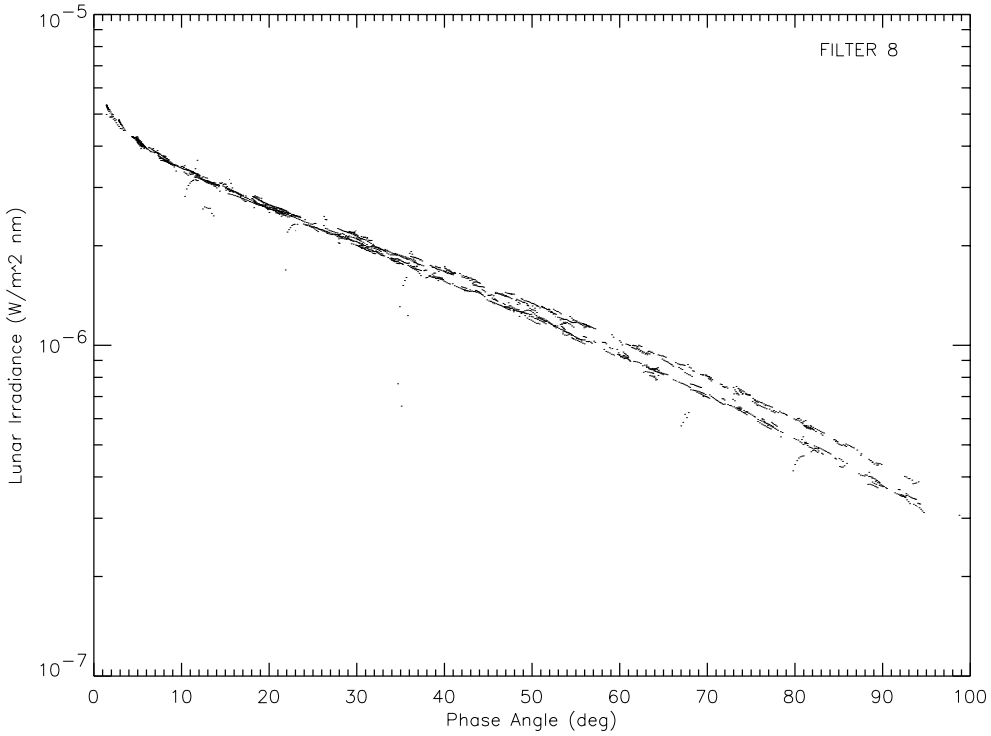

Figure 5. Lunar Irradiance vs. Phase Angle. All ROLO lunar irradiance data in filter 8 (550 nm) with phase angle $\leq 100^\circ$ are shown, including outlier points which may be traced to unfavorable observing conditions and are culled in later analysis. The two branches show the difference in luminosity at waxing and waning lunar phases.

Lunar absolute irradiances are derived from the lunar image integrations, corrected to standard distance:

$$\mathcal{I} = (I_\oslash \cdot C_L \cdot C_{ext}) \cdot \Omega_p \cdot f_D \tag{2}$$

where $I_\oslash$ is the instrumental irradiance sum in (DN/sec), C_L is the radiance calibration factor, C_{ext} is the nightly extinction correction, and Ω_p is the solid angle of one pixel. The irradiance correction factor to standard distance is:

$$f_D = \left(\frac{D_\oslash}{384400}\right)^2 \cdot D_\odot^2 \tag{3}$$

where $D_\oslash$ is the Moon–observer distance in km and $D_\odot$ is the Moon–Sun distance in AU. Figure 5 shows ROLO lunar irradiance measurements in the 550-nm band plotted as a function of phase angle. The apparent split toward larger phase angles results from the higher abundance of mare regions in the western lunar hemisphere, which gives a diminished relative intensity after Full Moon.

4.2. Lunar Radiometric Model

The development of fit coefficients in the ROLO lunar photometric model is done in dimensionless units of reflectance. The conversion between irradiance and effective disk reflectance is:

$$A_{\oslash\lambda} = \frac{\mathcal{I}_{\oslash\lambda}}{\Omega_\oslash \cdot S_{\odot\lambda}/\pi} \tag{4}$$

where $A_\oslash$ is the disk-equivalent albedo (full Lambert lunar disk), λ is the effective wavelength of a band, $\Omega_\oslash$ is the solid angle of the Moon and $S_\odot$ is the solar spectral irradiance, the latter two at standard distances. This conversion involves a solar spectral irradiance model, which may have significant uncertainties in some wavelength regions;

however, the direct dependence on solar model cancels to first order as long as the same model is used in going from irradiance to reflectance and back.

The ROLO photometric model currently used has the form:

$$\ln A_\lambda = \sum_{i=0}^{m} a_i |g|^i + \sum_{j=1}^{n} p_j g^{2j-1} + c_a \theta + c_b \phi \qquad + c_o(1/|g| - 1/c_g) \quad \text{for} \quad |g| < c_g \tag{5}$$

where g, θ and ϕ are the observer phase angle and selenographic latitude and longitude. The polynomial in absolute phase angle has m =3, and the asymmetry polynomial has n=3 (fifth degree). The opposition effect (enhanced backscattering) term has a width c_g = 8.5°. The a, p, and other c coefficients are fitted independently for each band. For a preliminary modeling run which fitted 37857 lunar images, the mean absolute deviation in logarithm of irradiance was 0.0116 or 1.16%. However, this says nothing about the accuracy of the absolute scale for each band.

4.3. Adjustment of Irradiance Model Absolute Scale

The preliminary ROLO lunar irradiance model exhibits sharp structure in reflectance that does not appear in the reflectance spectra of returned Apollo samples, which show only weak and broad spectral features. However, no individual Apollo sample is representative of the entire Moon, and all Apollo soil samples have been "disturbed" such that the change in material spectral properties with depth over the first few mm that is probable on the Moon (due to interplay between energetic atomic bombardment and gardening by impacting micro-meteorites) cannot be recovered. Nonetheless, linear combinations of the reflectance spectra of an Apollo soil sample and an Apollo breccia follow the trends of the disk-equivalent albedo produced by ROLO models.

This roughness of the ROLO model spectrum is addressed by determining a scaling constant for each band that will yield a reflectance spectrum which matches a linear combination of spectra of returned Apollo soil and breccia samples.[13] Figure 6 shows the effective disk albedo spectrum at 10° phase angle and zero libration found from the ROLO model, along with a synthetic spectrum derived from Apollo samples with a 96/4 mix of soil and breccia and an overall scale factor of 0.86. The ratio of the synthetic spectrum to the ROLO spectrum is the adjustment used to scale the ROLO model results.

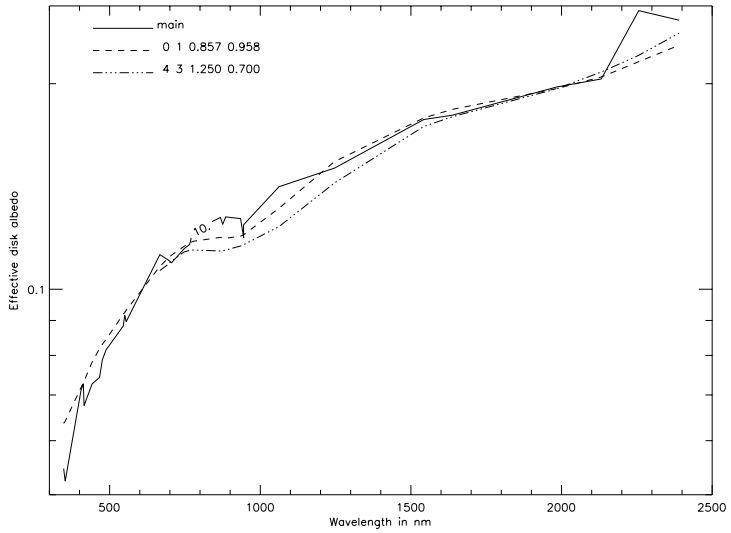

Figure 6. Comparison of Lunar Spectra. The solid line is the ROLO lunar irradiance model at 10° phase angle and zero libration, expressed as effective disk albedo. The dashed line is a scaled linear combination of two Apollo returned samples[13] convolved with the ROLO filter transmissions; the fraction of soil is 96%. The ratio of these two curves is used for scaling factors for the lunar irradiance model to remove the spectral jitter. The dash-triple-dot line is a scaled linear combination of telescopic spectra from dark and bright locations near the lunar crater Aristarchus.[14]

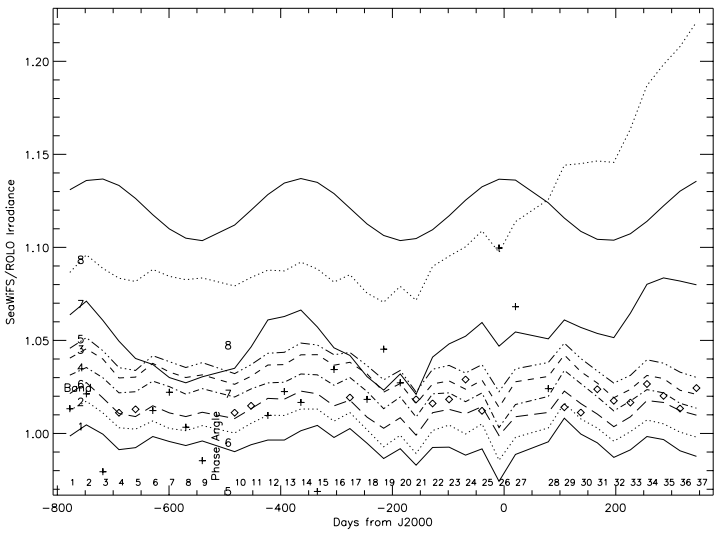

Figure 7. Chronologic trends in the discrepancy between SeaWiFS calibration and the ROLO lunar irradiance model. The abscissa indicates days from January 0.5, 2000. Bands are indicated near day –760. The time-dependent part of the SeaWiFS calibration included dates through the 20^{th} observation of the Moon (indicated by the number along the bottom of the plot). Band 8 (upper dotted line) has continued to lose responsivity after that time. The heavy line represents the inverse of the heliocentric range (offset from 1.0), showing an initial correlation to the calibration ratio, especially in Band 7 (intermediate-weight solid line). The rapid month-to-month correlated variations are attributed to poor knowledge of the oversampling factor.[15,17] Lunar phase angles are indicated by plus signs (positive) and diamonds (negative); a guide to phase angle is indicated near day –500.

5. SPACECRAFT IRRADIANCE COMPARISONS

Because of the strong dependence of lunar irradiance on geometric angles, observations by spacecraft cannot be compared directly to ROLO images. Rather, the lunar irradiances based on the spacecraft instrument calibration are compared with the lunar radiometric model. The geometric processing involved for comparison of spacecraft lunar images is described in an accompanying paper.[15]

SeaWiFS has made observations of the Moon on a monthly basis, usually near a phase angle of 7.5° in both waxing and waning phases. The calibration coefficients used here for processing SeaWiFS lunar images are those of Ref. 16, Table 4, which are based on analysis of the first 20 SeaWiFS observations of the Moon. This calibration contains time-dependent linear terms for all bands and quadratic terms in time for Bands 7 and 8. We have applied this calibration also to observations 21 through 37.

Figure 7 shows the calibration discrepancy ratio for SeaWiFS measurements of irradiance of the Moon relative to the ROLO model. The time rate of change of response in the calibration coefficients for Bands 1–6 is small (less than $\sim 10^{-5}$ per day); the comparison here suggests that those rates (the lower 6 curves) are slightly underestimated. The high-frequency correlated jitter in these 6 curves is probably due to the difficulty in determining the oversampling factor from images that are only 6×20 pixels.[17] The trends shown in Fig. 7 suggest that the rate of sensitivity loss in Bands 7 and 8 seen during the first two years slowed thereafter. Band 7, and to a lesser extent the other bands, show an inverse correlation with distance from the Sun, thought to be an effect of instrument temperature.[18] These variations, which are at the $\frac{1}{2}\%$ level for most bands, probably could not have been detected without the lunar observations.

ACKNOWLEDGMENTS

The ROLO project is supported by Goddard Space Flight Center as part of the NASA Mission to Planet Earth under NASA contract S-41359-F. SeaWiFS images were provided by Gene Eplee.

REFERENCES

1. Spectralon is a trademark of Labsphere Inc., 231 Shaker St, N. Sutton, NH 03260
2. J. M. Anderson, "Modeling Atmospheric Component Abundances to Determine ROLO Atmospheric Extinction", ROLO Internal Document, December 1998 (unpublished)
3. A. Berk, L. S. Bernstein, and D. C. Robertson, "MODTRAN: A moderate resolution model for LOWTRAN 7," Technical Report GL-TR-89-0122, Air Force Geophysics Laboratory, Hanscom AFB, MA.
4. G. P. Anderson, *et al.*, "FASCODE/MODTRAN/LOWTRAN: Past/present/future," in *18th Annual Review Conference on Atmospheric Transmission Models, 6–8 June 1995*, U.S. Air Force Geophysics Laboratory, 1995, as provided in MODTRAN 3.5 documentation
5. G. W. Lockwood and D. T. Thompson, "Atmospheric Extinction: The Ordinary and Volcanically Induced Variations, 1972–1985," *Astron. J.*, **92**, pp. 976–985, 1986
6. A. Landolt, "*UVBRI* Photometric Standard Stars Around the Celestial Equator," em Astron. J., **88**, pp. 439–460, 1983
7. H. H. Kieffer and R. L. Wildey, "Establishing the Moon as a Spectral Radiance Standard," *J. Atmos. and Ocn. Tech.*, **13**, pp. 360–375, 1996
8. S. F. Biggar, "Calibration of a visible and near-infrared portable transfer radiometer," *Metrologia*, **35**, pp. 701–706, 1998
9. D. S. Hayes, "Stellar Absolute Fluxes and Energy Distributions from 0.32 to 4.0 microns," in *Calibration of Fundamental Stellar Quantities; Proceedings of the Symposium, Como, Italy, May 24–29, 1984*, pp. 225–252, D. Reidel Publishing Co. (Dordrecht), 1985
10. D. W. Strecker, E. F. Erickson, and F. C. Witteborn, "Airborne stellar spectrophotometry from 1.2 to 5.5 microns — absolute calibration and spectra of stars earlier than M3," *Astrophys. J. Supp.*, **41**, pp. 501–512, 1979
11. `HTTP://CFAKU5.HARVARD.EDU/stars/VEGA/`
12. F. Castelli and R. L. Kurucz, "Model atmospheres for Vega," *Astron. Astrophys.*, **281**, pp. 817–832, 1994
13. C. M. Pieters and J. F. Mustard, "Exploration of crustal/mantle material for the Earth and Moon using reflectance spectroscopy," *Rem. Sens. Environ.*, **24**, pp. 151–178, 1988
14. P. G. Lucey, B. R. Hawke, C. M. Pieters, J. W. Head, and T. B. McCord, "A compositional study of the Aristarchus region of the Moon using near-infrared spectroscopy," *J. Geophys. Res.*, **91**, pp. D344–D354, 1986
15. H. H. Kieffer, P. Jarecke, and J. Pearlman, "Lunar Calibration Observations by the EO-1 Hyperion Imaging Spectrometer," *these proceedings*, **4480-31** , 2001
16. R. A. Barnes and C. R. McClain, "The calibration of SeaWiFS after two years on-orbit," *Proc. SPIE*, **3870**, pp. 214–227, 1999
17. H. H. Kieffer, J. M. Anderson, and K. J. Becker, "Radiometric Calibration of Spacecraft using Small Lunar Images," *Proc. SPIE*, **3870**, pp. 193–205, 1999
18. R. A. Barnes, R. E. Eplee, G. M. Schmidt, F. S. Patt, and C. R. McClain, "The Calibration of SeaWiFS. Part 1: Direct Techniques," *Applied Optics*, in press, 2001